



Study on the fluoride adsorption of various apatite materials in aqueous solution

Shan Gao, Jing Cui, Zhenggui Wei*

School of Chemistry and Environmental Science, Nanjing Normal University, Nanjing 210097, PR China

ARTICLE INFO

Article history:

Received 9 May 2009

Received in revised form 4 August 2009

Accepted 3 September 2009

Available online 9 September 2009

Keywords:

Adsorption

Apatite

n-HAp

Bone meal

Defluoridation capacity

ABSTRACT

The aim of this study was to evaluate the defluoridation efficiencies of various sorbents in aqueous solution. These sorbents include synthetic nano-hydroxyapatite (n-HAp), biogenic apatite (bone meal), treated biogenic apatite (bone meal prepared by H_2O_2 oxidation) and geogenic apatite (rock phosphate), which were characterized by XRD, FTIR, TEM and SEM. It has been observed that the defluoridation capacities follow the order: n-HAp > BH_2O_2 > B > rock phosphate. The controlling factors, sorbent dose, initial fluoride concentration, pH, contact time and temperature were investigated. The defluoridation capacities increased with the increase in the initial fluoride concentration and contact time, decreased with the increase in the sorbent dose. The optimum pH range for removal of fluoride on various apatite sorbents was considered to be 5.0–6.0. The fluoride adsorption can be explained by Langmuir, Freundlich isotherms, and the adsorption kinetic data follow the pseudo-second-order model. Thermodynamic parameters such as ΔH° , ΔS° and ΔG° indicated that the adsorption on various apatite sorbents was spontaneous and endothermic. These results showed that bone meal is a promising material for fluoride adsorption.

© 2009 Elsevier B.V. All rights reserved.

1. Introduction

Fluoride in drinking water may have benefit for human health or on the contrary, which depends on the concentration of fluoride and the amount of that has been consumed [1]. The optimum concentration level of fluoride in drinking water for general good health is considered between 0.5 and 1.5 mg/L [2], while excess intake of fluoride may cause fluorosis, which is a kind of chronic disease of dental or skeletal problems, such as mottling of teeth in mild cases, softening bones and neurological damage in severe cases [3–6]. Excess fluoride in drinking water occurs in many countries due to its natural presence in the earth crust, or discharge by agricultural and industrial activities, such as steel, aluminium, glass, electroplating [7–9].

Various treatment technologies were proposed or applied to remove the excess fluoride from drinking water before consumption, and these technologies were based on the principle of precipitation, the ion exchange, the membrane or the adsorption processes [10–14]. Among these methods, adsorption is a simple and attractive one because of its high efficiency and easy handling. In recent years, much effort has been devoted to investigate and develop new fluoride sorbent using various synthetic, naturally occurring and waste materials from various industries and requires little processing [15].

Generally, nano-hydroxyapatite (n-HAp) as synthetic apatite was found to be a suitable sorbent for fluoride because of their low costing, availability and higher adsorption efficiency as previously reported by the authors [16]. Bones consist about 30% of organic compounds by weight, most of them are fibrous protein collagen, while the remaining 70% represent inorganic phase, which are composed of defect, poorly crystalline, cation and anion substituted HAPs [17]. A form of apatite is the principal mineral constituent of bone [18]. Therefore, animal bones represent a source of biogenic apatite. It would be an extension for bone meal to apply in the field of defluoridation, as they have been used in studies on the removal of the cadmium, lead and zinc [19]. However, as to our knowledge, the adsorption and the removal of fluoride by bone meal has not been reported.

In this paper, bone meal was used as sorbent material to remove fluoride from polluted water. Studies were carried out in synthetic fluoride solutions with the objective of establishing process parameters. Experiments were carried out with synthetic nano-hydroxyapatite (n-HAPs prepared by solution-precipitation method), biogenic apatite (bone meal) and treated biogenic apatite (bone meal prepared by H_2O_2 oxidation). The geogenic apatite (rock phosphate) was also studied for comparison.

2. Results and discussion

2.1. Characterization of sorbents

Bone meal and treated bone meal by H_2O_2 oxidation obtained from the preparation route described in experimental section were

* Corresponding author. Tel.: +86 25 84395014; fax: +86 25 84395815.
E-mail address: zgwei@njau.edu.cn (Z. Wei).

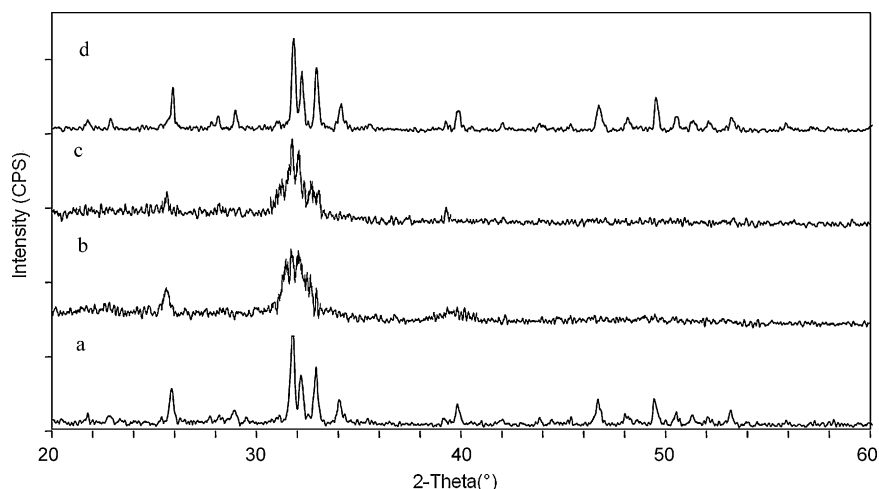


Fig. 1. XRD patterns of (a) n-HAp, (b) B, (c) BH₂O₂, (d) rock phosphate.

denoted as B and BH₂O₂, respectively. The XRD patterns of investigated samples (Fig. 1), confirmed that HAp was the main crystalline phase as reported by Gao [16], while a broad and intense background was associated with collagen and other organic compounds (Fig. 1b and c).

The structure of the samples was analyzed using FTIR spectroscopy as shown in Fig. 2. The peaks at about 562, 601, 1040 and 1090 cm⁻¹ must be due to the PO₄³⁻ group. The OH⁻ bands at 3571 and 632 cm⁻¹ were clearly visible in the FTIR spectra of the n-HAp sample [20]. The broad band from 3700 to 2500 cm⁻¹, the most intensive in the spectra of B and BH₂O₂ sample, which are attributed to stretching modes of hydrogen bonded H₂O molecules. For the CO₃²⁻ group the peak positions are 870, 1410 and 1450 cm⁻¹. In addition, the spectra of sample B, at 1547–1559, 1242 and 666 cm⁻¹ amide I, II and III bands, were visible, which came from the organic phase. The band at 2923 cm⁻¹ occurred due to vibrations of –CH₂ groups, while at 1744 cm⁻¹ carbonyl groups were found. In the BH₂O₂ spectra, band at 1744 cm⁻¹ was removed, while other bands were present with the reduced intensities [21]. For the n-HAp and rock phosphate, the intensity of organic phase has decreased significantly.

The size and shape of n-HAp was measured by TEM. The SEM analysis was performed to understand the morphology of B, BH₂O₂ and rock phosphate. Fig. 3a indicates that the synthetic n-HAp samples were cylindrical rod like shape with homogeneous microstructure, 10–15 nm in diameter and 40–50 nm in length. Microstructure of bone meal was not homogenous as observed by SEM (Fig. 3b), which indicate that the organic compounds, mainly

fibrous protein collagen aggregates. The density of bone meal aggregates can be described as the number of protein aggregates per unit area [22]. As Fig. 3c shows, in the SEM image of BH₂O₂, some holes were clearly visible. These holes were to be explained as the organic fractions were primarily eliminated by H₂O₂ oxidation. Size (measured by manual analysis of the images), SEM image in Fig. 3d shows that rock phosphate appear by a distributed network of spherical beads (~2.5 μm) at a lamellar structure.

2.2. Effect of sorbent dose

The effect of sorbents (n-HAps, B, BH₂O₂, rock phosphates) dose on fluoride adsorption at pH 5.0 and fixed initial fluoride concentration (10 mg/L) is shown in Fig. 4. The amount of sorbent significantly influences the extent of fluoride adsorption. It is evident that fluoride removal (%) increased with the increase of sorbent doses while defluoridation capacity (amount of fluoride loaded per unit weight of sorbent, q_e) gradually decreased for the same. The extent of fluoride removal was greatly increased to 90.94% (2.27 mg/g) with 0.1 g/25 mL of n-HAp, 86.45% (2.18 mg/g) of B, and 88.01% (2.20 mg/g) of BH₂O₂. The results showed that n-HAp toward F⁻ has good adsorption properties, sample B (bone meal) and BH₂O₂ also have high fluoride removal. Bone meal consists of organic compounds (mainly fibrous protein collagen) and inorganic phase composed of HAp. After treatment by H₂O₂, the organic compounds were almost removed and sample BH₂O₂ has more inorganic phase than sample B, so the defluoridation decreased in the order: BH₂O₂ > B. Furthermore, higher sorbent dose results in lower q_e (mg/g) value. Similar behavior has also been reported previously for other sorbents [5,23–25]. But for the rock phosphates, because of the slow rate of release of OH⁻, exhibit very low fluoride removal efficiency. Therefore, 0.1 g/25 mL was chosen as the optimum dose and used as the further study.

2.3. Effect of initial fluoride concentration

Fig. 5 shows the effect of initial fluoride concentration on the equilibrium defluoridation capacity (q_e) and fluoride removal (%) on various apatite sorbents. The results revealed that, the q_e value increases while the percentage removal decreases with the increase in the initial fluoride concentration. This indicates that sorbent surface offer a limited number of active sites, compared with the relatively large number of active sites required for the high initial fluoride concentration [26]. For n-HAp, B and

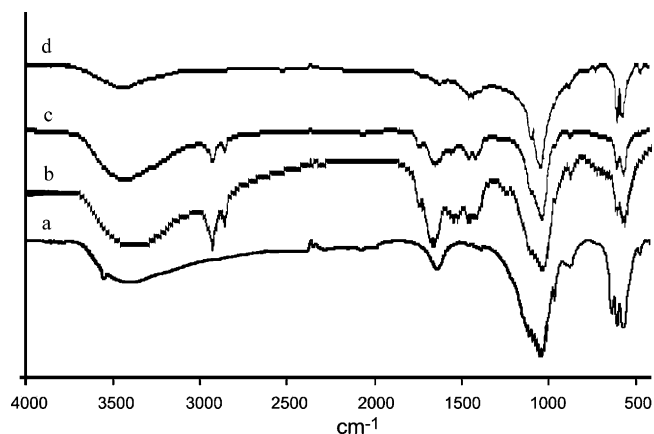


Fig. 2. FTIR spectra of (a) n-HAp, (b) B, (c) BH₂O₂, (d) rock phosphate.

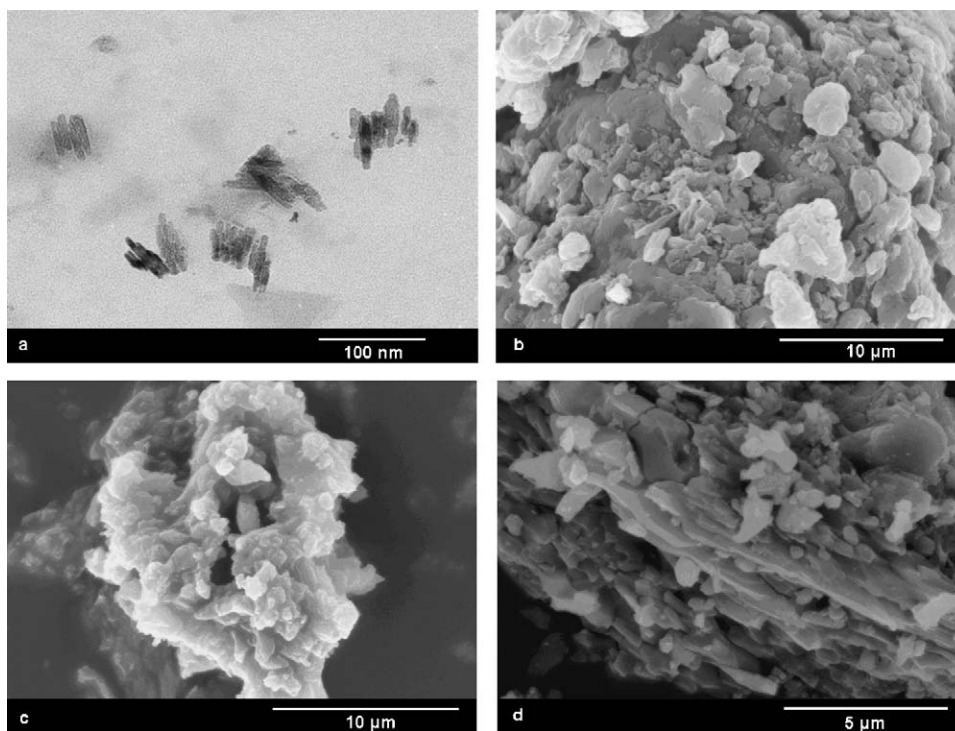


Fig. 3. TEM of (a) n-HAp and SEM of (b) B, (c) BH_2O_2 , (d) rock phosphate.

BH_2O_2 , experimentally obtained q_e values were in the range 0.702–6.161 mg/g, while affinity of the investigated sorbents towards fluoride decreased in the following order: n-HAp > BH_2O_2 > B. It was also clear to see that there is no distinct difference in q_e values on rock phosphate.

2.4. Effect of pH

The pH of the medium is one of the important variables which significantly affect the extent of adsorption of fluoride. The adsorption of fluoride on sorbents (n-HAps, B, BH_2O_2 , rock phosphates) was studied at different initial pH between 2.0 and 11.0. Fig. 6 shows the effect of the initial solution pH on the fluoride adsorption onto different sorbents at the given conditions. For n-HAp, the maximum fluoride removal (87.07%) was recorded at pH 2.0 and showed gradual decreasing trend with increase in the pH. This is in agreement with fluoride removal studies on synthetic n-HAp by other report [16]. While for B and BH_2O_2 samples, the fluoride removal first dramatically increased to 78.95% and 84.35% at pH 5.06, and then slightly decreased to 61.12% and 72.84% at pH 11.0. This is consistent with the results reported by other researchers for different types of sorbents [1,24,27]. The relatively lower fluoride removal in the acidic range ($\text{pH} < 5.0$) may be due to the formation of weakly ionized hydrofluoric acid, which reduces availability of free fluoride for adsorption. The reduction of fluoride removal in alkaline pH range should be attributed to competition of hydroxyl ions with fluoride for adsorption sites because of similarity in fluoride and hydroxyl ions in charge and ionic radius. Similar findings have also been reported earlier [1,24]. However, the details for the effect of pH on fluoride adsorption mechanism need to be further studied.

For rock phosphate, the sorbent exhibited negligible fluoride removal in all the pH ranges studied. This may be as a result of the weakly solubility of rock phosphate. For all sorbents, further adsorption experiments were considered to be in the initial pH range 5.0–6.0.

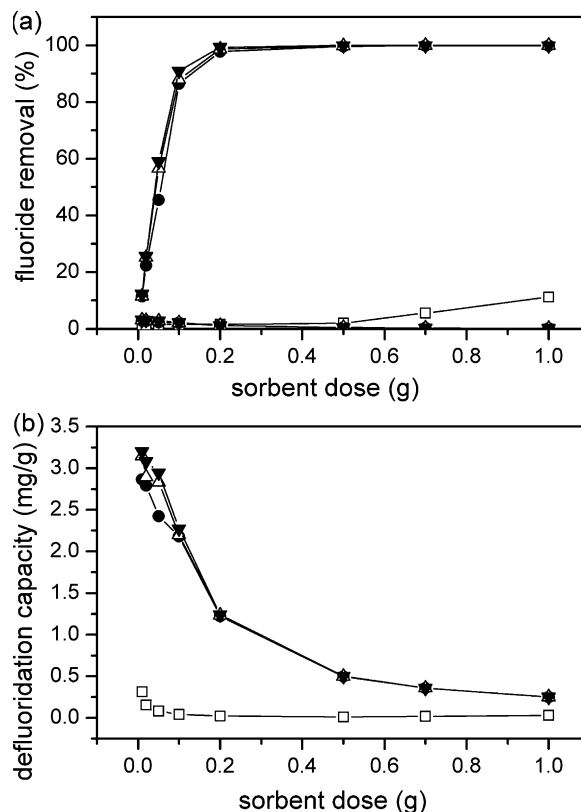


Fig. 4. Effect of sorbent dose: (a) fluoride removal (%), (b) amounts of fluoride sorbed. Sorbents: (▼) n-HAp, (●) B, (△) BH_2O_2 , (□) rock phosphate (initial fluoride concentration: 10 mg/L, contact time: 100 min, pH: 5.0, and at 298 K).

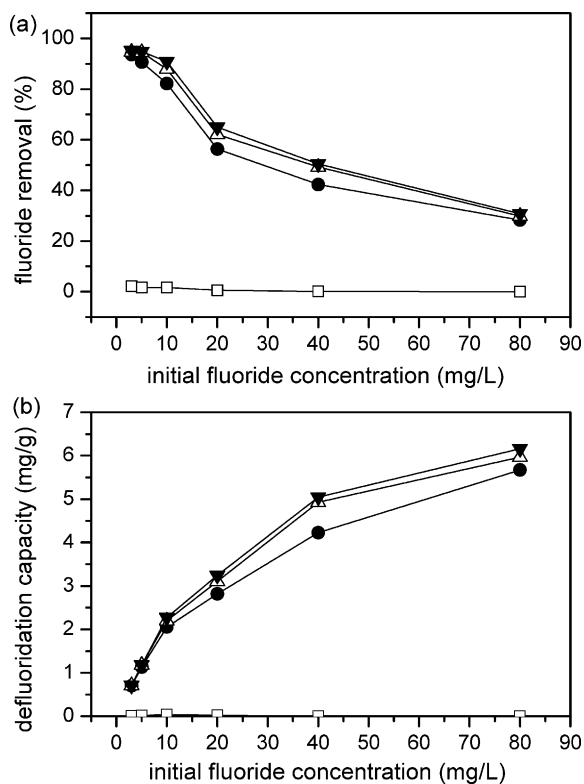


Fig. 5. Effect of initial fluoride concentration: (a) fluoride removal (%), (b) amounts of fluoride sorbed. Sorbents: (▼) n-HAp, (●) B, (△) BH₂O₂, (□) rock phosphate (dose: 0.1 g/25 mL, contact time: 100 min, pH: 5.0, and at 298 K).

2.5. Effect of contact time

The adsorption of fluoride by various apatite sorbents as a function of contact time is presented in Fig. 7. The adsorption occurred in two steps: an initial fast step which lasted for 10–20 min, and a slower second phase which continued until the end of the experimental period. The equilibrium was established almost after 100 min, so a contact time of 100 min was selected for further testing. It was observed that the amounts of fluoride adsorbed increased with the increase in contact time. The n-HAp recorded a maximum defluoridation capacity of 2.305 mg F[−]/g when compared with B (2.219 mg F[−]/g) and BH₂O₂ (2.221 mg F[−]/g). While for the rock phosphate, the defluoridation efficiency is very low and no remarkable changes were observed for longer contact time, which also indicated that the adsorption rate of fluoride on rock phosphate was much slower than that of n-HAp and bone meal sorbents for fluoride. The data obtained from this experiment were further used successfully to evaluate the kinetics of the adsorption process.

2.6. Effect of temperature

Fig. 8 shows the adsorption of fluoride on various apatite sorbents obtained at four different temperatures (298, 308, 318 and 328 K) and at pH 5.0. Obviously, the adsorption of fluoride on various sorbents increased with the rise of the temperature in the range of 298–328 K. This phenomenon might also indicate that the adsorption of fluoride onto n-HAp, B, BH₂O₂ and rock phosphate samples was endothermic in nature.

2.7. Adsorption isotherms

Analysis of equilibrium data is important for developing an equation that can be used to compare different sorbents under

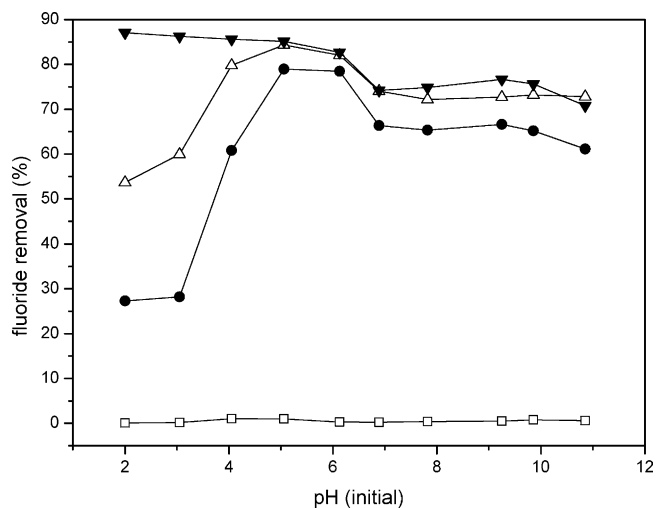


Fig. 6. Effect of pH on the removal extent of fluoride. Sorbents: (▼) n-HAp, (●) B, (△) BH₂O₂, (□) rock phosphate (initial fluoride concentration: 10 mg/L, dose: 0.1 g/25 mL, contact time: 100 min, and at 298 K).

different operational conditions and to design and optimize an operating procedure [28]. The fluoride adsorption capacity of various sorbents was evaluated using two different isotherms namely Langmuir and Freundlich isotherms. In this study, the Langmuir and Freundlich equilibrium isotherm models were used to describe the equilibrium between the adsorbed fluoride on various sorbents and fluoride in solution at the constant temperatures [29].

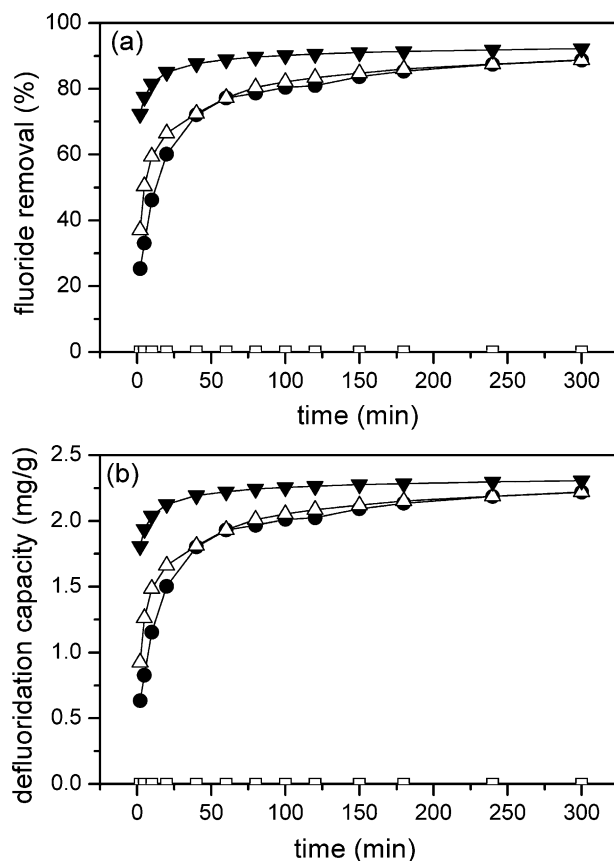


Fig. 7. Effect of contact time: (a) fluoride removal (%), (b) amounts of fluoride sorbed. Sorbents: (▼) n-HAp, (●) B, (△) BH₂O₂, (□) rock phosphate (initial fluoride concentration: 10 mg/L, dose: 0.1 g/25 mL, pH: 5.0, and at 298 K).

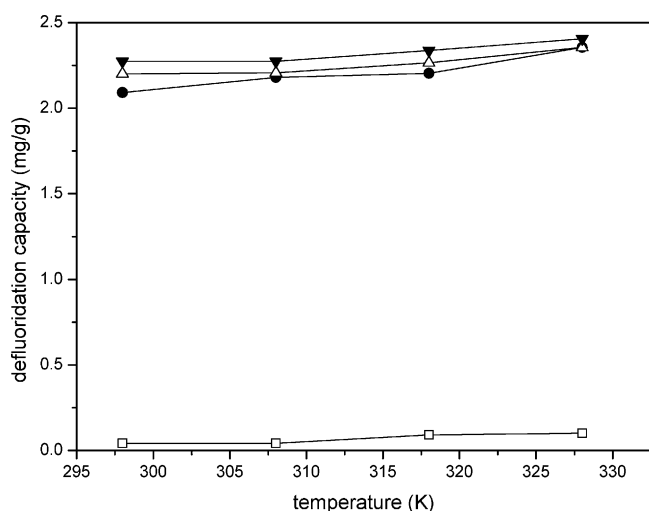


Fig. 8. Effect of temperature on the removal extent of fluoride. Sorbents: (▼) n-HAp, (●) B, (△) BH₂O₂, (□) rock phosphate (initial fluoride concentration: 10 mg/L, dose: 0.1 g/25 mL, pH: 5.0, and contact time: 100 min).

Table 1

Isotherms with linear forms and their plots.

Isotherms	Linear form	Plot
Langmuir	$Q = Q^0 b C_e / (1 + b C_e)$	$1/Q = 1/Q^0 + 1/Q^0 b C_e$
Freundlich	$Q = K_F C_e^{1/n}$	$\log Q = \log K_F + \log C_e / n$

Langmuir isotherm [30] model is listed in Table 1. The adsorption capacity (Q^0) is the amount of adsorbate at complete monolayer coverage (mg/g), it gives the maximum adsorption capacity of sorbent, Q is the equilibrium fluoride concentration on the sorbent (mg/g), C_e is the equilibrium concentration of fluoride in solution (mg/L), and b (L/mg) is the Langmuir isotherm constant that relates to the energy of adsorption. The respective values of Q^0 and b were calculated from the slope and intercept of the plot $1/Q$ vs. $1/C_e$ and Table 2 lists the results.

With Freundlich isotherm model [31] the linear form is presented in Table 1. K_F is the empirical constant of Freundlich isotherm (L/mg) and $1/n$ is the adsorption intensity. The values of Freundlich isotherm constants $1/n$ and K_F were calculated from the slope and intercept of the plot $\log Q$ vs. $\log C_e$. Values of resulting parameters and regression coefficients (R^2) are listed in Table 2. The results of their linear regression were used to find out fitted model from them.

By comparing the results presented in Table 2, it can be seen that the plots of Langmuir and Freundlich models have provided a reliable description of the experimental data (except for the rock phosphate sample), which are further confirmed by the extremely high values of the coefficient of determination. The applicability of both isotherms to n-HAp, B and BH₂O₂. The R_L (a dimensionless separation factor) values computed for the present system are provided in Table 3. The R_L values between 0 and 1 indicate favorable adsorption for all the initial concentrations. The essential

Table 3

Equilibrium parameter, R_L .

Sample	C_0 (mg/L)	3	5	10	20	40	80
n-HAp	0.202	0.132	0.071	0.037	0.019	0.009	
B	0.289	0.196	0.109	0.057	0.03	0.015	
BH ₂ O ₂	0.311	0.213	0.119	0.063	0.033	0.017	

C_0 is the initial fluoride concentration.

features of the Langmuir isotherm can be expressed in terms of R_L . As indicated in Table 2, the adsorption capacity (measured by K_F) of the sorbents decreases in the order n-HAp (1.764 L/mg) > BH₂O₂ (1.662 L/mg) > B (1.413 L/mg) > rock phosphate (0.034 L/mg), which indicated that the adsorption capacity of n-HAp is the largest [32]. Further the value of intensity of adsorption (n) is greater than unity signified that the forces within the surface layer are attractive [33].

According to the Langmuir model, a single adsorbate is retained in only one molecular layer and Freundlich equation deals with physicochemical adsorption on heterogeneous surfaces [34]. The results in this study indicate that both monolayer adsorption and heterogeneous surfaces conditions exist under the experimental conditions used. But for the rock phosphate, low values of R^2 , and the parameters n and b were negative, showing that the adsorption system is unfavorable.

2.8. Adsorption kinetics

The contact time experimental results can be used to study the rate determining step in the adsorption process, as shown by Weber and Morris [35]. The adsorption kinetics of fluoride from synthetic solutions was carried out at pH 5.0 and 10 mg/L of fluoride, and the results are shown in Fig. 7b. The pseudo-first-order [36] and pseudo-second-order [37] models were tested to interpret the experimental data of investigated adsorption processes.

Pseudo-first-order model:

$$\frac{dq_t}{dt} = K_1(q_1 - q_t) \rightarrow \log(q_1 - q_t) = \log q_1 - \frac{K_1 t}{2.303} \quad (1)$$

Pseudo-second-order model:

$$\frac{dq_t}{dt} = K_2(q_2 - q_t)^2 \rightarrow \frac{t}{q_t} = \frac{1}{K_2 q_2^2} + \frac{t}{q_2} \quad (2)$$

where q_t (mg/g) is the uptake of fluoride at time t , t (min) is the shaken time, q_1 (mg/g) the maximum adsorption capacity for pseudo-first-order, and K_1 (min^{-1}) is the pseudo-first-order rate constant for fluoride in adsorption process, respectively. And q_2 (mg/g) is the maximum adsorption capacity for pseudo-second-order. K_2 ($\text{g}/(\text{mg min})$) is the pseudo-second-order rate constant for fluoride in adsorption process. The linear plots of fluoride adsorption kinetics to the two models and the calculated kinetic parameters are given in Table 4.

From Table 4, it can be seen that both high correlation coefficients ($R^2 > 0.999$) and good agreement between experimental q_{exp} and

Table 2

Isotherm parameters of samples at 298 K.

Sample	Langmuir			Freundlich			
	Q_0 (mg/g)	b (L/mg)	R^2	$1/n$	n	K_F (L/mg)	R^2
n-HAp	4.575	1.316	0.9909	0.337	2.966	1.764	0.9544
B	4.99	0.821	0.9353	0.35	2.857	1.413	0.9833
BH ₂ O ₂	6.849	0.74	0.9737	0.341	2.937	1.662	0.9637
Rock phosphate	0.014	<0	0.105	<0	<0	0.034	0.2588

Table 4

Lagergren constants for adsorption of fluoride onto various apatite sorbents at 298 K.

Sample	q_{exp}	Pseudo-first-order rate contents			Pseudo-second-order rate contents		
		K_1	q_1	R^2	K_2	q_2	R^2
n-HAp	2.305	0.016	0.288	0.9475	0.242	2.311	0.9999
B	2.219	0.014	0.839	0.9650	0.062	2.247	0.9993
BH ₂ O ₂	2.221	0.015	1.074	0.9490	0.043	2.267	0.9993

Table 5

Thermodynamic parameters for the adsorption of fluoride on various apatite sorbents at different temperatures.

Sample	ΔS^0 (J/Kmol)	ΔH^0 (J/Kmol)	ΔG^0 (kJ/mol)			
			298 K	308 K	318 K	328 K
n-HAp	91.738	25.441	−1.897	−2.814	−3.732	−4.649
B	97.124	28.545	−0.398	−1.369	−2.34	−3.312
BH ₂ O ₂	75.346	21.261	−1.192	−1.946	−2.699	−3.452
Rock phosphate	50.451	28.86	13.826	13.321	12.817	12.312

calculated q_2 values indicated that the pseudo-second-order kinetic model can represent the adsorption kinetics. It is worth pointing out that, even though the values of R^2 for the pseudo-first-order model are between 0.947 and 0.965, experimental q_{exp} and calculated q_1 values are not in agreement with each other. Therefore, it could be suggested that the adsorption of fluoride onto the n-HAp, B and BH₂O₂ was not a first-order reaction.

2.9. Thermodynamic investigations

The thermodynamic parameters such as the enthalpy change (ΔH^0), the entropy change (ΔS^0) and the free energy change of the adsorption (ΔG^0) were calculated in same way as the related researches did in literature [38–40].

The values of ΔH^0 and ΔS^0 have been computed from the slope and intercept of the straight line of plots of $\log(q_e/C_e)$ vs. $1/T$ (Fig. 9). The values of these thermodynamic properties are given in Table 5. The results indicate that ΔG^0 values are negative (except for the rock phosphate sample) which mean that the reaction is spontaneous, while the positive ΔG^0 values indicate non-spontaneous nature of fluoride adsorption reaction with rock phosphate and, that has governed with the gain of energy from surroundings [41,42]. The free energy of the process at all temperatures was negative and changed with the rise in temperature. Positive values of ΔH^0 indicate the endothermic nature of the adsorption process. This suggests that

an increase in the temperature is tended to increase the adsorption capacity [43]. As indicated in Table 5, the positive ΔS^0 values for the present system indicate that increased randomness at the solid/solution interface during the adsorption of fluoride onto various apatite sorbents.

3. Conclusions

The results of this study have demonstrated that biogenic apatite (bone meal) is a kind of suitable precursor materials for the production of high defluoridation capacity from aqueous solution. In this research, bone meal was treated with an oxidation agent in order to partially remove the organic components with preservation of the poor apatite phase crystallinity. Fluoride adsorption efficiencies by various apatite sorbents (synthetic n-HAp, B, BH₂O₂ and rock phosphate) were compared at different experimental conditions.

It was found that the amount of fluoride adsorbed on sorbents depends on sorbent dose, initial fluoride concentration, pH, contact time and temperature. Increase in the initial fluoride concentration or contact time could result in the increase of the defluoridation capacity. However, the higher sorbent dose might lead to the decrease of the defluoridation capacity. Optimal adsorption was obtained in the wide initial pH range 5.0–6.0.

Except for the rock phosphate, the results obtained from adsorption isotherms on other apatite sorbents were well described by the Langmuir and Freundlich model. The adsorption kinetic study revealed that the adsorption process followed the pseudo-second-order equation. The adsorption reaction on various apatite sorbents was found to be spontaneous and endothermic. The calculated maximum defluoridation capacities, which decreased in the order: n-HAp (2.311 mg/g) > BH₂O₂ (2.267 mg/g) > B (2.247 mg/g) > rock phosphate, which indicated that the biogenic apatite or treated biogenic apatite have comparable defluoridation capacities compared with the synthetic n-HAp. The proposed bone meal sorbent for defluoridation is an inexpensive material.

4. Experimental

4.1. Materials

The rock phosphates were purchased from Plant Nutrition Labs, Nanjing Agricultural University. Calcium nitrate, ammonium phosphate, sodium fluoride and all other chemicals used were of analytical grade and used without further purification. Stock

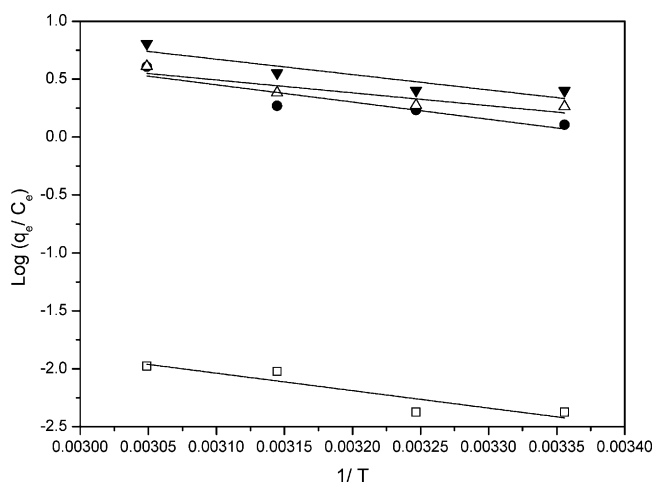


Fig. 9. $\log(q_e/C_e)$ vs. $1/T$ for the adsorption of fluoride from aqueous solution. Sorbents: (▼) n-HAp, (●) B, (△) BH₂O₂, (□) rock phosphate.

solution of fluoride was prepared by dissolving 2.21 g of sodium fluoride in 1 L distilled water.

4.2. Preparation of bone sorbents

The bone meal used was obtained in powder form, from a commercial supplier, and is identical to that used as a garden fertilizer. The bone meal was divided into two parts. First part, denoted as B. Second part, treated with an oxidation agent (30% H_2O_2), was in order to remove the organic phase of the bone, which was named as BH_2O_2 . 0.5 g of bone meal was placed in a 250 ml digestion tube and 3.5 ml of 30% H_2O_2 was added. The H_2O_2 solution was changed daily and heated up to the boiling temperature, three times a day. The process was stopped after 7 days, when no visible reaction occurred, and the sample was dried for 24 h, at 80 °C [21].

4.3. Preparation of n-HAP

n-HAPs were prepared by solution-precipitation method using $\text{Ca}(\text{NO}_3)_2 \cdot 4\text{H}_2\text{O}$ and $(\text{NH}_4)_2\text{HPO}_4$ as starting materials and ammonia solution as agents for pH adjustment. A suspension of $\text{Ca}(\text{NO}_3)_2 \cdot 4\text{H}_2\text{O}$ was vigorously stirred and a solution of $(\text{NH}_4)_2\text{HPO}_4$ was slowly added dropwise to the $\text{Ca}(\text{NO}_3)_2 \cdot 4\text{H}_2\text{O}$ solution. In all experiments the pH of $\text{Ca}(\text{NO}_3)_2 \cdot 4\text{H}_2\text{O}$ solution by ammonia solution was 11.0. Then the precipitated HAP has been removed from solution by centrifugation method at the rotation speed of 3000 rpm. The powder was dried at 80 °C and then calcined at 100 °C for 1 h [20].

4.4. Adsorption experiments

The adsorption studies have been carried out at fluoride concentrations of 10 mg/L as initial fluoride concentration. A given amount of sorbents (0.1 g) have been placed in 100 mL PVC conical flask and mixed with 25 mL of stock solution and shaken for 100 min on a shaker followed by centrifugation for 15 min. Then the solid was separated by filtration through a membrane with 0.45 μm pore size and the residual fluoride was measured immediately by Orion ion selective electrode. A pH/ISE meter (Orion Model, EA 940 Expandable Ion Analyzer) equipped with combination fluoride-selective electrode (Orion Model 96-09) was employed for the measurement of fluoride ions concentration. The pH value of solutions was adjusted with 0.1 M HNO_3 or 0.1 M NaOH . All measurements were performed in triplicate and experimental errors were found below 5%.

The defluoridation studies were conducted for the optimization of various experimental conditions like sorbent dose, initial fluoride concentration, pH, contact time and temperature. Kinetic studies of sorbent were carried out at a constant temperature of 298 K. The thermodynamic parameters of the adsorption were established by conducting the experiments at 298, 308, 318 and 328 K in a temperature controlled mechanical shaker. The defluoridation capacity q_e onto sorbent (n-HAPs, B, BH_2O_2 , rock phosphates) was calculated from the difference between the initial C_0 and the residual concentration C_t in solution as follows:

$$q_e = C_0 - C_t \frac{V}{m} \quad (3)$$

m and V are sorbent mass and the volume of the contaminated solution, respectively. Experiments were conducted at 298 K.

4.5. Characterization of sorbents

All prepared sorbents were analyzed by X-ray diffraction (XRD), using Cu Ka ($\lambda = 1.5405 \text{ \AA}$) radiation on a Rigaku D/max-rB X-ray powder diffractometer. The patterns were registered in the 2θ

range from $20^\circ < 2\theta < 60^\circ$ with a scanning step size of 0.02° and an acquisition time of 4 s/step.

FTIR spectral examinations were performed by Bomem MB 100 FTIR spectrometer. The spectra were recorded in the $4000\text{--}500 \text{ cm}^{-1}$ region, collecting 10 scans per spectrum, with a resolution of 4 cm^{-1} , using potassium bromide pellet technique. Pellets were prepared using 1 mg sample/15 mg KBr.

The size and morphology of the samples were recorded with a Hitachi H-7650 transmission electron microscope (TEM) and a Hitachi Model S-3000 N scanning electron microscope (SEM) operating at 15 kV.

Acknowledgements

This work is supported by the National Programs for High Technology Research and Development of China (no. 2007AA10Z406), the Research Fund for the Doctoral Program of Higher Education (no. 20070307051), SRF for ROCS, SEM, the Foundation for Talent Recommendation Program of Nanjing Normal University, and the Leading Academic Discipline Program, 211 Project for Nanjing Normal University (the 3rd phase).

References

- [1] M.G. Sujana, R.S. Thakur, S.B. Rao, J. Colloid Interface Sci. 206 (1998) 94–101.
- [2] WHO, Fluorine and Fluorides, Environmental Health Criteria, vol. 36, WHO, Geneva, 1984.
- [3] Y. Wang, E.J. Reardon, Appl. Geochem. 16 (2001) 531–539.
- [4] H. Lounici, L. Addour, D. Belhocine, H. Grib, S. Naicolas, B. Bariou, Desalination 114 (1997) 241–251.
- [5] M. Srimurali, A. Pragathi, J. Karthikeyan, Environ. Pollut. 99 (1998) 285–289.
- [6] M. Hichour, F. Persia, J. Sandeaux, C. Gavach, Sep. Purif. Technol. 18 (2000) 1–11.
- [7] Z. Amor, S. Malki, M. Taky, B. Bariou, N. Mameri, A. Elmidaoui, Desalination 120 (1998) 263–271.
- [8] S.M. Hasany, M.H. Chaudhary, Appl. Radioactive Isot. 47 (4) (1996) 467–471.
- [9] D. Cohen, H.M. Conrad, Desalination 117 (1998) 19–35.
- [10] W.G. Nawlakhe, D.W. Kulkarni, B.N. Pathak, K.R. Bulusu, Indian J. Environ. Health 17 (1975) 26–65.
- [11] M. Yang, Y. Zhang, B. Shao, R. Qi, H. Myoga, J. Environ. Eng. 127 (2001) 902–907.
- [12] Y. Ku, H.-M. Choi, W. Wang, Sep. Sci. Technol. 37 (2002) 89–103.
- [13] M. Hichour, F. Persia, J. Sandeaux, C. Gavach, J. Membr. Sci. 212 (2003) 113–121.
- [14] S.D. Faust, O.M. Aly, Adsorption Processes for Water Treatment, Butterworth, Stoneham, MA, 1987, p. 299.
- [15] S. Bailey, T.R. Olin, M.A. Dean, Water Res. 33 (1999) 2469–2479.
- [16] S. Gao, R. Sun, Z.G. Wei, H.Y. Zhao, H.X. Li, F. Hu, J. Fluorine Chem. 130 (2009) 550–556.
- [17] T.S.B. Narasaraaju, D.E. Phebe, J. Mater. Sci. 31 (1996) 1–21.
- [18] C. Rey, in: Z. Amjad (Ed.), Calcium Phosphates in Biological and Industrial Systems, Kluwer Academic Publishers, Boston, MA, 1998, pp. 217–245.
- [19] I.R. Sneddon, M. Orueetxebarria, M.E. Hodson, P.F. Schofield, E. Valsami-Jones, Environ. Pollut. 144 (2006) 816–825.
- [20] I. Mobasherpour, M. Soulati Heshajin, A. Kazemzadeh, M. Zakeri, J. Alloys Compd. 430 (2007) 330–333.
- [21] S. Dimović, I. Smčiklas, I. Plečič, D. Antonović, M. Mitrić, J. Hazard. Mater. 164 (2009) 279–287.
- [22] L.V.D. Berg, Y. Rosenberg, Martinus, A.J.S. van Boekel, M. Rosenberg, F.V.D. Velde, Food Hydrocoll. 23 (2009) 1288–1298.
- [23] M. Agarwal, K. Rai, R. Shivastav, S. Dass, J. Clean. Prod. 11 (2003) 439–444.
- [24] A.M. Raichur, M.J. Basu, Sep. Purif. Technol. 24 (2001) 121–127.
- [25] V.K. Gupta, I. Ali, V.K. Saini, Water Res. 41 (2007) 3307–3316.
- [26] B. Stephen Inbaraj, N. Sulochana, Indian J. Chem. Technol. 9 (2002) 201–208.
- [27] D.P. Das, J. Das, K.M. Parida, J. Colloid Interface Sci. 274 (2003) 213–220.
- [28] R. Yao, F.P. Meng, L.J. Zhang, D. Ma, M.L. Wang, J. Hazard. Mater. 165 (2009) 454–460.
- [29] K.L. Lin, J.Y. Pan, Y.W. Chen, R.M. Cheng, X.C. Xu, J. Hazard. Mater. 161 (2009) 231–240.
- [30] I. Langmuir, J. Am. Chem. Soc. 38 (1916) 2221–2295.
- [31] H.M.F. Freundlich, Z. Phys. Chem. 57A (1906) 385–470.
- [32] J.Q. Jiang, C. Cooper, S. Quki, Chemosphere 47 (2002) 711–716.
- [33] J. Budhraj, M. Singh, J. Indian Chem. Soc. 81 (2004) 573–575.
- [34] A.K. Yadav, C.P. Kaushik, A.K. Haritash, A. Kansal, N. Rani, J. Hazard. Mater. 128 (2006) 289–293.
- [35] W.J. Weber, J.C. Morris, J. Saint. Eng. Div. ASCE 89 (1963) 31–33.
- [36] S. Lagergren, Handlingar 24 (1898) 1–39.
- [37] Y.S. Ho, G. McKay, Process Biochem. 34 (1999) 451–465.
- [38] E. Malkoc, Y. Nuhoglu, J. Hazard. Mater. 127 (2005) 120–128.
- [39] E. Malkoc, Y. Nuhoglu, M. Dundar, J. Hazard. Mater. 138 (2006) 142–151.
- [40] M. Dundar, C. Nuhoglu, Y. Nuhoglu, J. Hazard. Mater. 151 (2008) 186–195.
- [41] A.A.M. Daifullah, S.M. Yakout, S.A. Elrefy, J. Hazard. Mater. 147 (2007) 633–643.
- [42] A. Ozcan, E.M. Oncu, S. Ozcan, Colloids Surf. A: Physicochem. Eng. Aspects 277 (2006) 90–97.
- [43] S. Sun, A. Wang, J. Hazard. Mater. 131 (2006) 103–111.